

Figure S1: Sensitivity of high and low multiplicity cell-free virus infection to TFV. MT-4 cells were either mock infected with growth medium (top row), or infected with fluorescently labeled HIV (YFPNL4-3) at high m (middle row) or low m (bottom row). Cells were pre-incubated for 24 hours with TFV and infected in the presence of the drug at the concentrations shown above the plots. Two days after infection, 2×10^5 MT-4 cells were analyzed by flow cytometry for YFP fluorescence. Gated cells had a high 535nm (YFP specific fluorescence) to 590nm (auto-fluorescence) ratio. Numbers above gate are the percent of YFP positive cells in the total population.

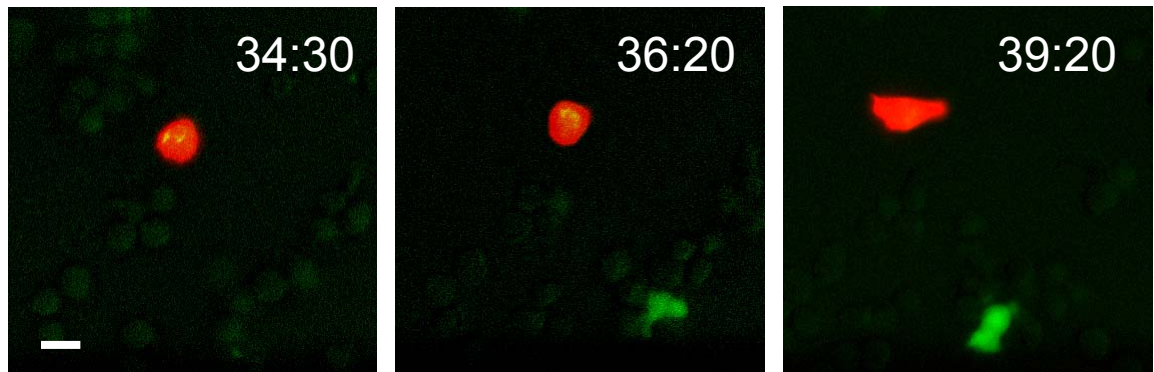
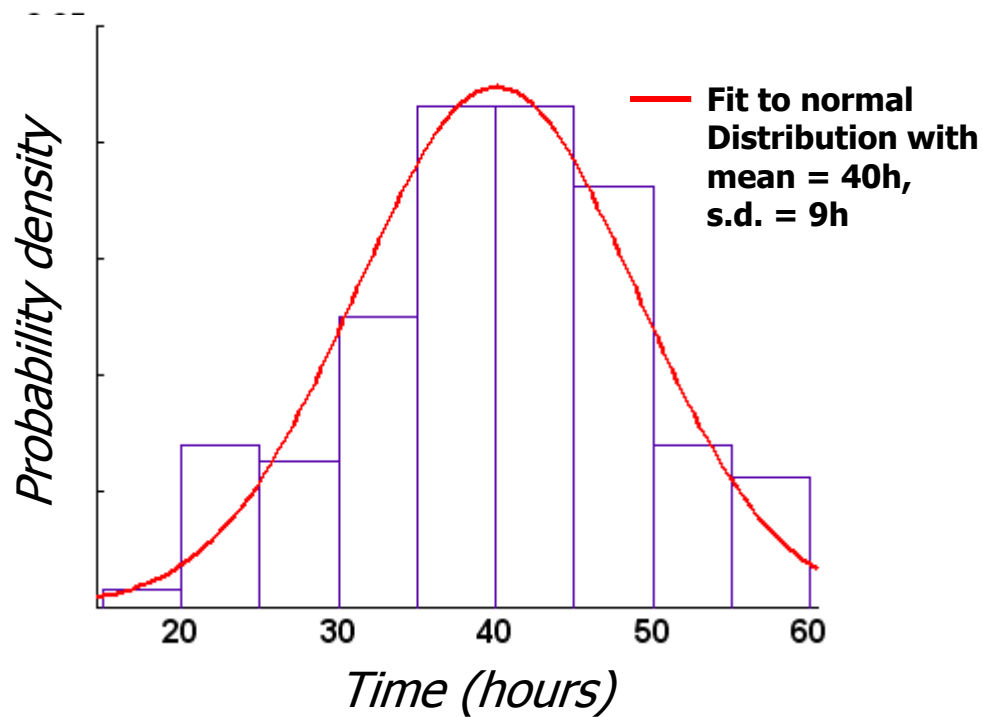
a**b**

Figure S2: Time to GFP expression in HIV infected Rev-CEM reporter cells. The length of a full viral cycle was approximated by the time to Tat and Rev dependent GFP expression. At time 0, infected MT-4mCherry cells were added to uninfected Rev-CEM cells and infection imaged with time-lapse microscopy at 37°C with 5% CO₂ for a period of 58 hours. a) Appearance of GFP in a Rev-CEM reporter cell (green). Time in hours indicated in top right corner. Red cell is infected MT-4mCherry donor. Scale bar is 20 μm. b) histogram of GFP expression times in 144 Rev-CEM cells. Fusions between donors and targets were excluded from analysis. Red curve represents fit of normal distribution with a mean = 40 hours and s.d. = 9 hours. Standard errors on the fit were ± 0.7 on the mean and ± 0.5 on s.d., with RMSE = 0.64.

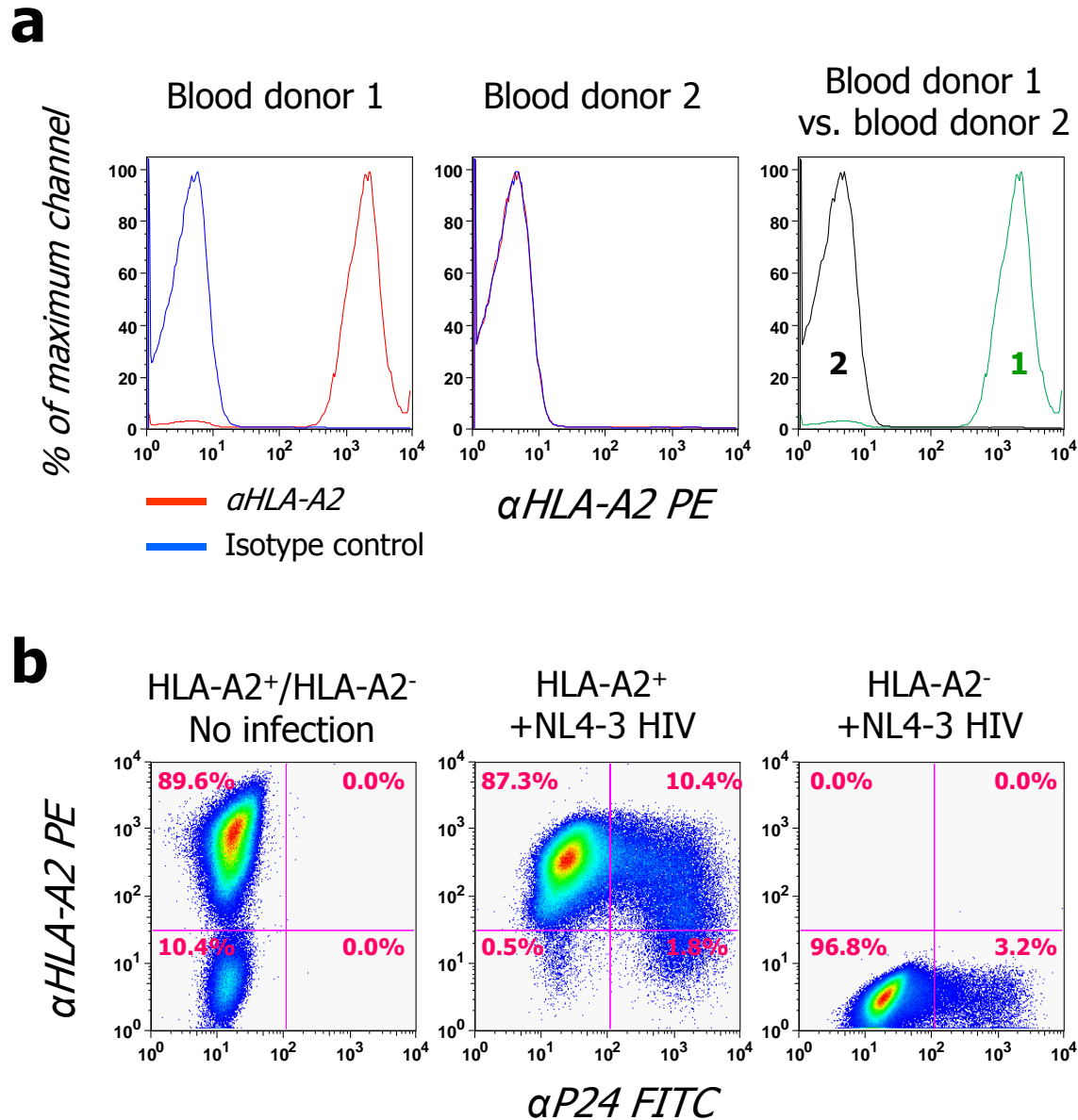


Figure S3: Controls for PBMC-to-PBMC infection. a) PBMC with HLA-A2⁺ (left plot) or HLA-A2⁻ (middle plot) serotype. Red line shows staining with α HLA-A2, PE conjugated antibody, and blue line shows staining with isotype control. α HLA-A2 stained PBMC from the HLA-A2⁺ serotype (1) and HLA-A2⁻ serotype (2) are compared in the rightmost plot. b) Uninfected and single positive controls. HLA-A2⁺ and HLA-A2⁻ PBMC were mixed in the absence of infection (left plot). In all experiments, the number of added HLA-A2⁻ PBMC, which were used as donor cells, was approximately tenfold less than the number of HLA-A2⁺ target cells. This was done to minimize transmissions with multiple infected donor cells infecting one target cell. To examine changes of HLA-A2 expression as a result of infection, HLA-A2⁺ PBMC (middle plot) or HLA-A2⁻ PBMC (right plot) were infected with cell-free NL4-3 HIV, and the number of infected cells quantified by α P24, FITC conjugated antibody.

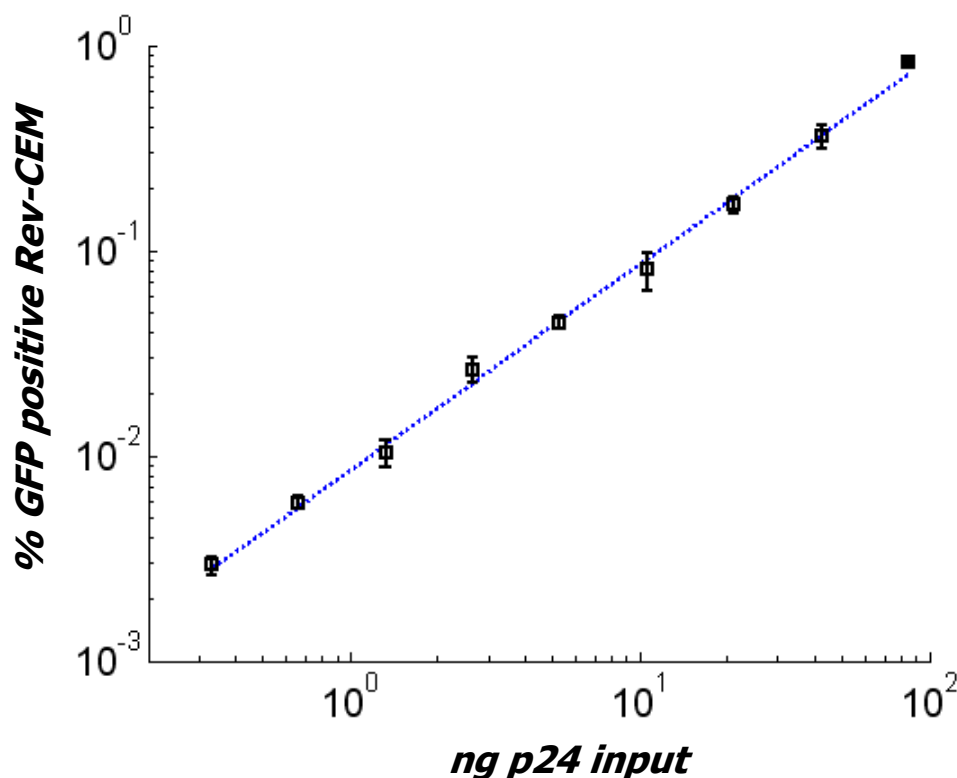


Figure S4: Relationship between viral input and number of GFP positive Rev-CEM reporter cells. We used Rev-CEM reporter T-cells as a target cell line. Cells of this line express GFP in the presence of HIV early proteins Tat and Rev. GFP is under viral long terminal repeat promoter regulation, and Tat leads to an increased number of full length transcripts from this promoter. GFP coding sequence is also flanked by a splice donor and splice acceptor and contains a Rev response element. The GFP coding sequence is therefore spliced out in the nucleus unless Rev shuttles the unspliced viral RNA out of the nucleus before splicing can occur, thus leading to GFP expression. These reporter cells enabled us to use unlabelled (hence unattenuated) HIV. To test for linearity of expression as a function of virus dose, 2 ml of cells at 2×10^5 cells/ml were infected with serially diluted virus stock. Dashed line represents fit of $y = 10^{(m \log(x) + \log(b))}$, with slope $m = 0.5$, $R^2 > 0.99$. 1 ng p24 was found to contain 8×10^6 HIV genomes (Methods). Means \pm s.d. of replicates ($n = 3$).

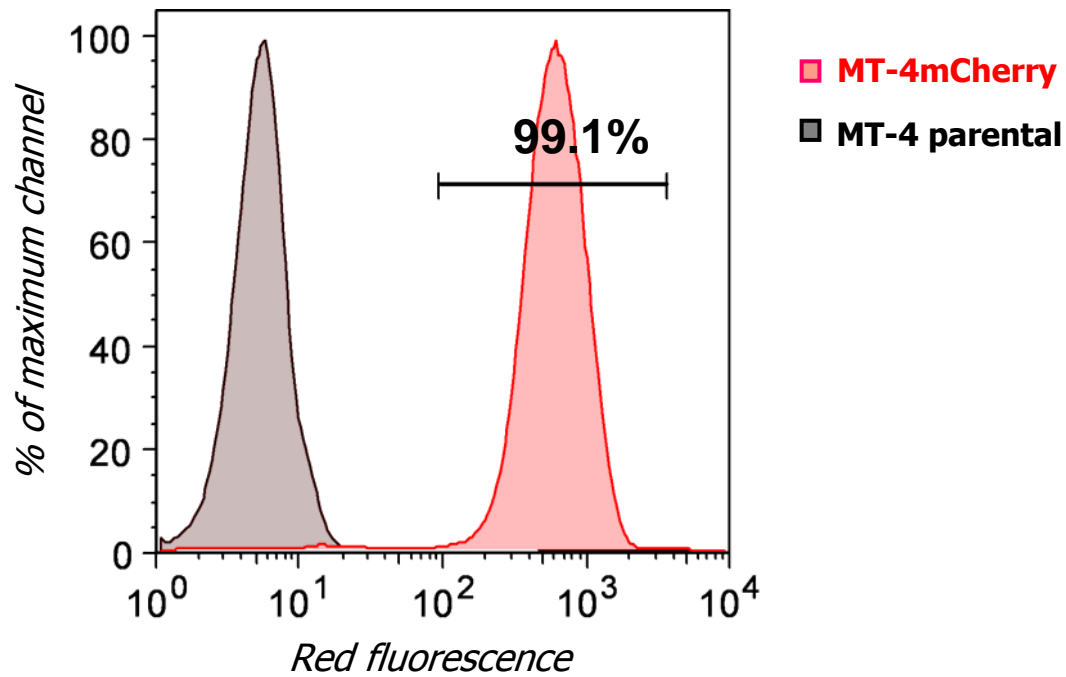
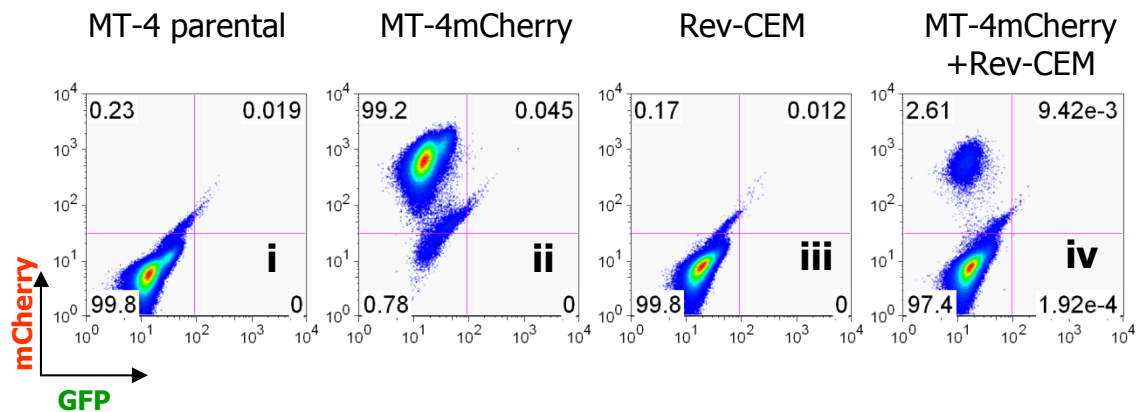
a**b**

Figure S5: Fraction of mCherry positive cells in the MT-4mCherry cell line. a) MT-4mCherry cells (red histogram) versus parental MT-4 cells (grey histogram). b) Dot plot analysis of (i) MT-4 parental line, (ii) MT-4mCherry (iii) uninfected Rev-CEM target cells (iv) uninfected Rev-CEM target cells mixed with MT-4mCherry donor cells. Numbers represent percent of cells in each quadrant. Colors from red to blue represent decreasing cell density.

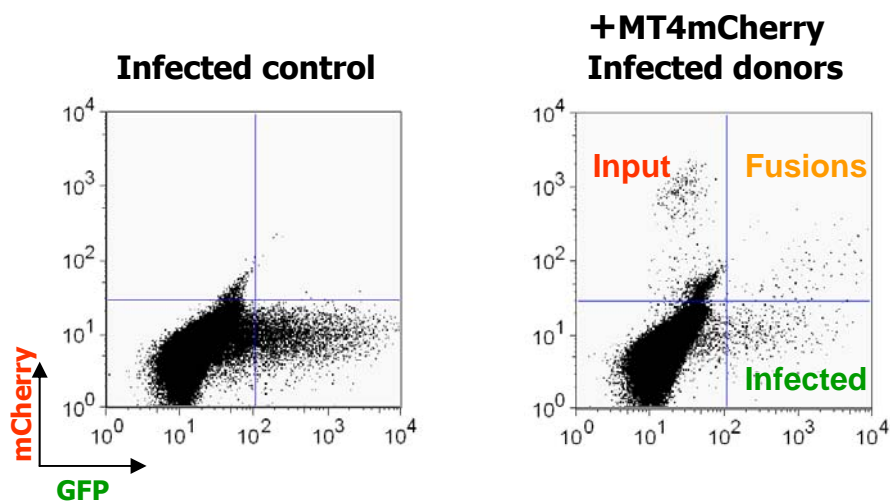
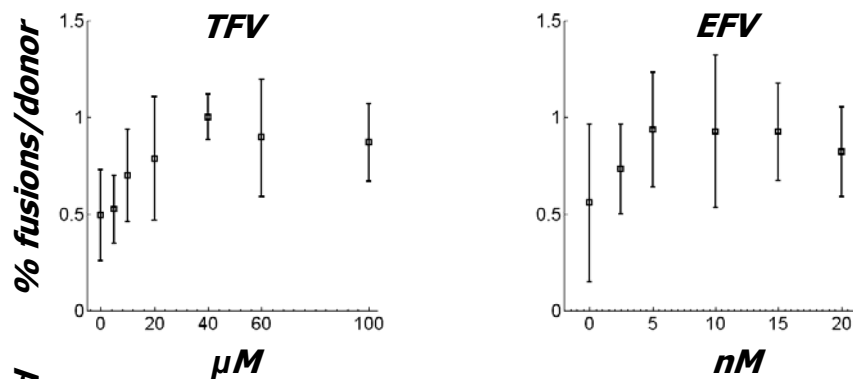
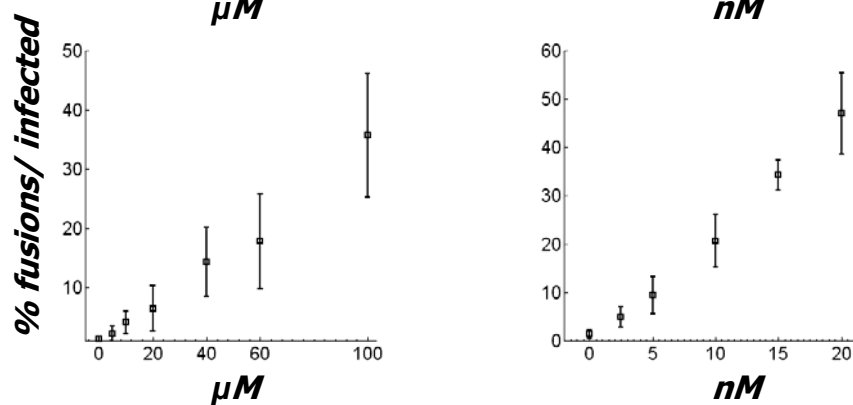
a**b****c**

Figure S6: Exclusion of donor-target cell fusions. a) Flow cytometry results show infection of Rev-CEM cells by cell-free virus (left plot) and infected MT-4mCherry donors (right plot). Upper right (UR) quadrant corresponds to GFP-mCherry double positive cells, lower right (LR) quadrant corresponds to GFP single positive cells, and upper left (UL) quadrant corresponds to MT-4mCherry donor cells. b) The ratio of the number of fused cells on day 2 post-infection to the number of MT-4mCherry donors on day 0 (UR/UL). c) The ratio of fused cells on day 2 to GFP single positive cells on day 2 (UR/LR). Squares are mean \pm s.d. of three consecutive independent inter-day experiments.

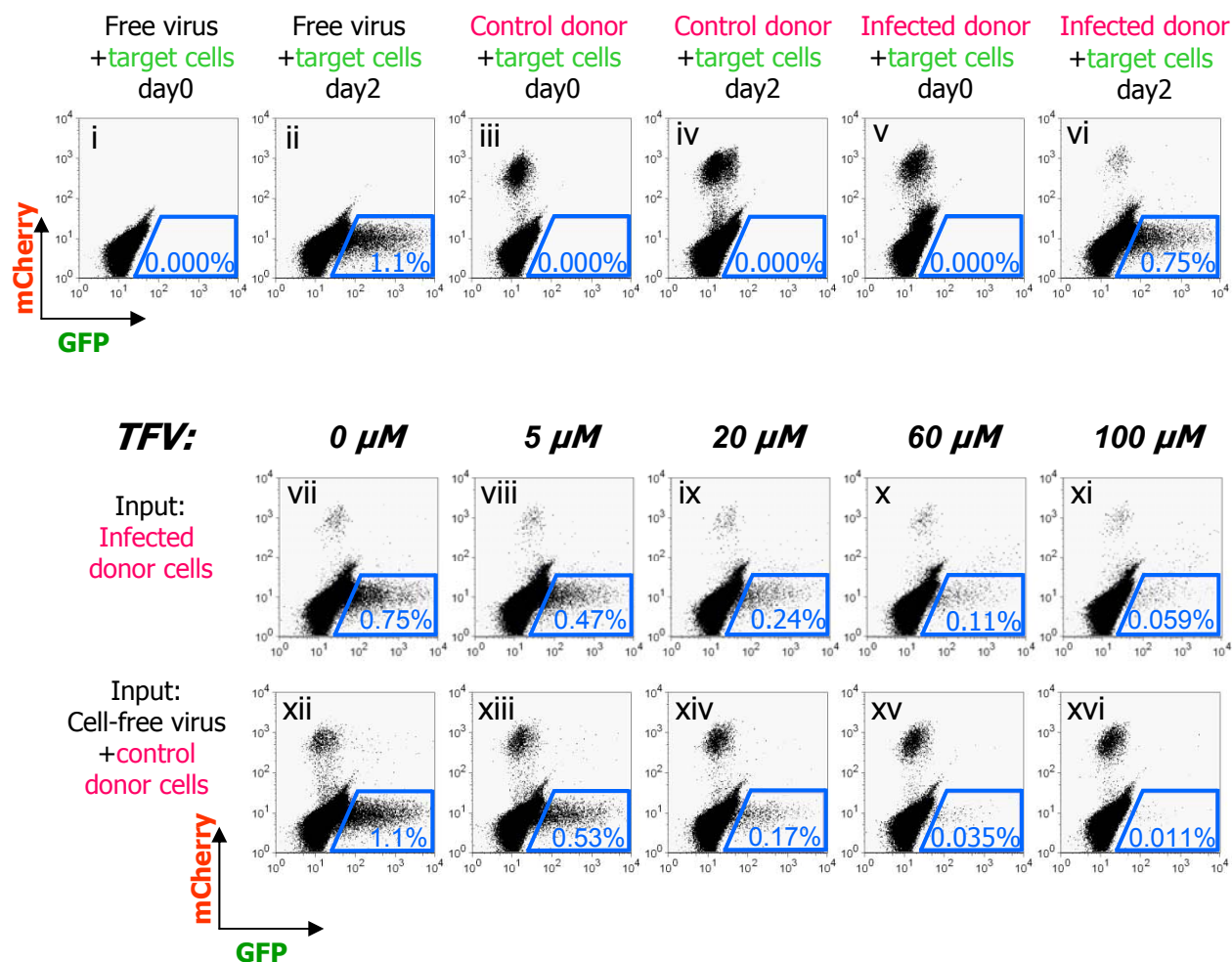


Figure S7: Drug sensitivity of HIV transmission from cocultured infected donor cells versus cell-free virus. Cells were infected with no virus, cell-free HIV or infected MT-4mCherry donor cells for 2 days and shown are flow cytometry plots of 5×10^5 cells with GFP versus mCherry fluorescence. Numbers are percent GFP positive Rev-CEM cells. i) uninfected Rev-CEM target cells before infection, ii) Rev-CEM cells infected with cell-free HIV day 2 post-infection, iii) uninfected MT-4mCherry donors + Rev-CEM targets on day 0, iv) uninfected MT-4mCherry donors + Rev-CEM targets on day 2. v) infected MT-4mCherry donors + Rev-CEM targets on day 0, vi) Infected MT-4mCherry donors + Rev-CEM targets on day 2, vii-xi) effect of TFV on day 2 post-infection when infection source is coculture with infected MT-4mCherry donors. xii-xvi) effect of TFV on day 2 post-infection when infection source is cell-free HIV. The fraction of MT-4mCherry donors was 1% on day 0 for control and infected MT-4mCherry cells. The reduction in the fraction of infected donor cells on day 2 is consistent with cell death of HIV infected cells.

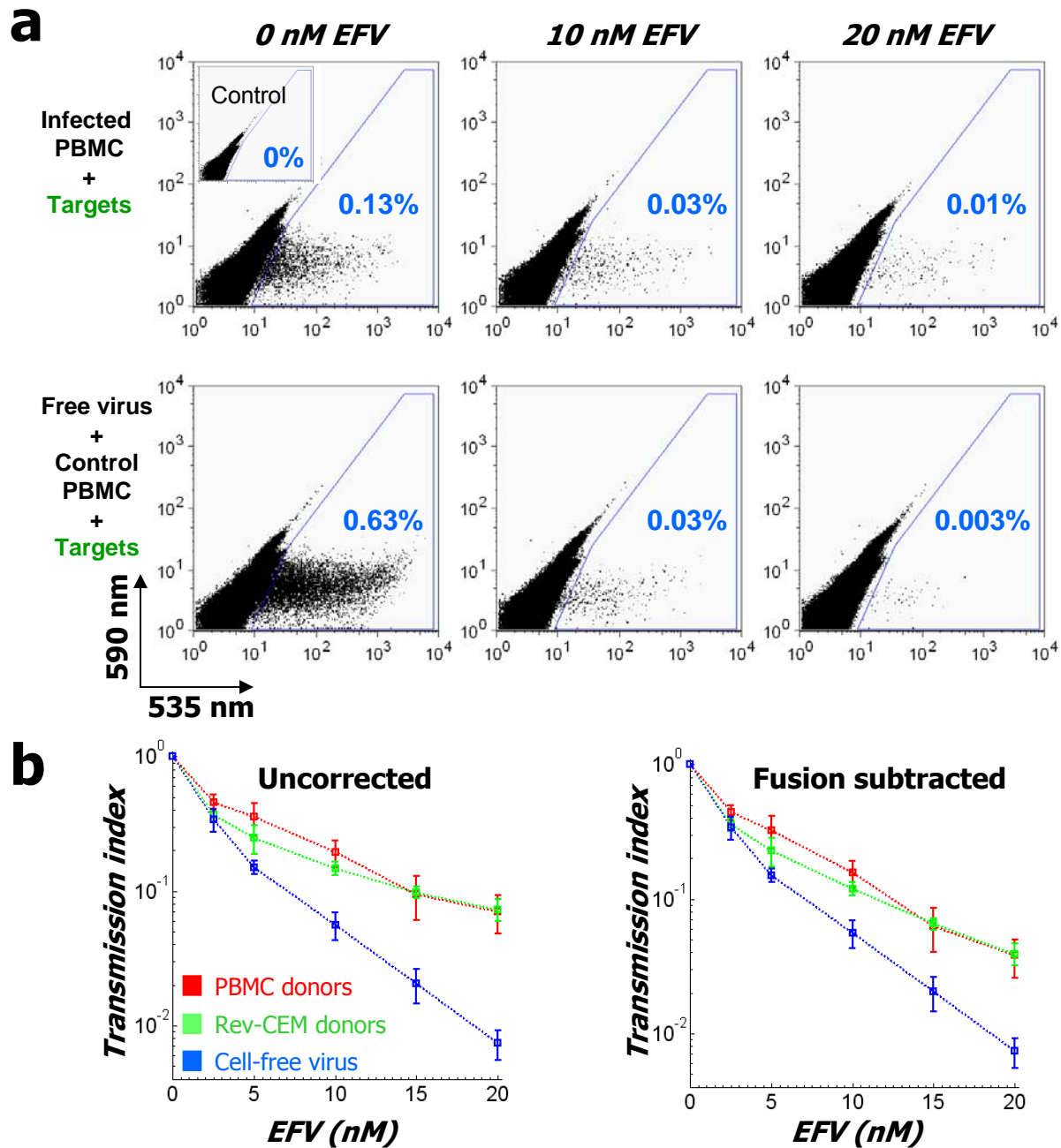


Figure S8: Drug sensitivity of cell-to-cell transmission from PBMC or Rev-CEM donors. a) FACS plots of 1.5×10^6 Rev-CEM target cells 2 days post-infection. Top row: infection source is infected PBMC donors with donor to target ratio of 1:50. Bottom row: infection source is cell-free virus. X-axis is 535 nm fluorescence (GFP specific), y-axis is 590 nm (auto-fluorescence). Numbers are percent GFP positive cells. b) Quantified transmission index for the infection of Rev-CEM target cells by infected PBMC donors (red squares), infected Rev-CEM donors (green squares), or cell-free virus (blue squares). Targets were Rev-CEM in all cases. Lines are guides for the eye. To differentiate between Rev-CEM donors and targets, targets were labeled with mCherry. Left graph is fusion uncorrected data, right graph shows fusion subtracted data, with fraction of fusions for each EFV concentration from Fig. S6c. Averages \pm s.d. of three consecutive independent inter-day experiments.

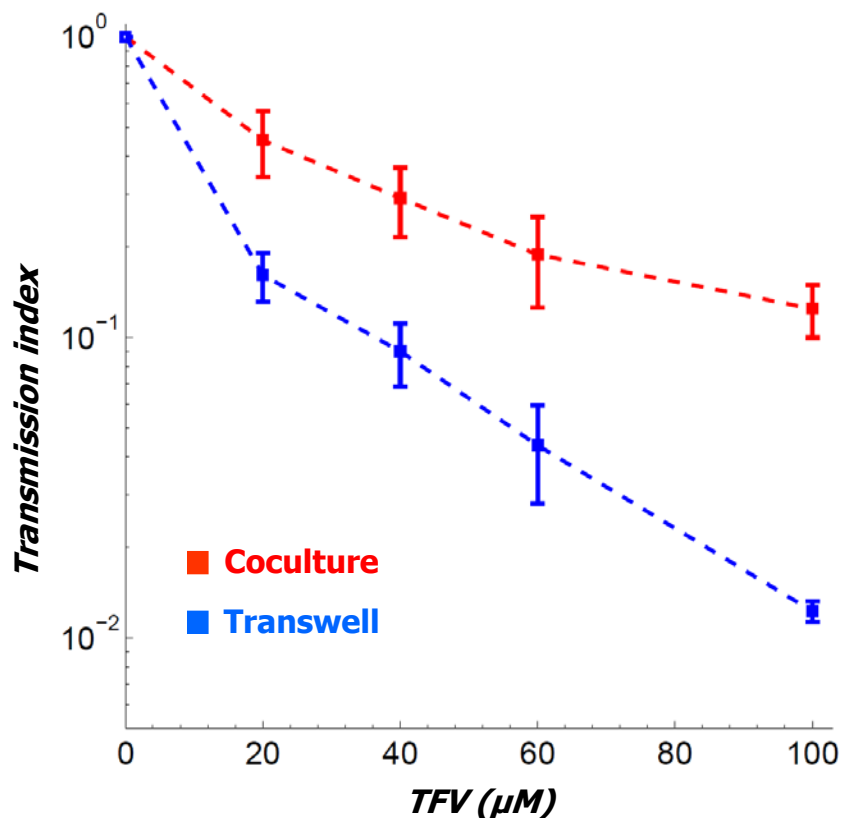
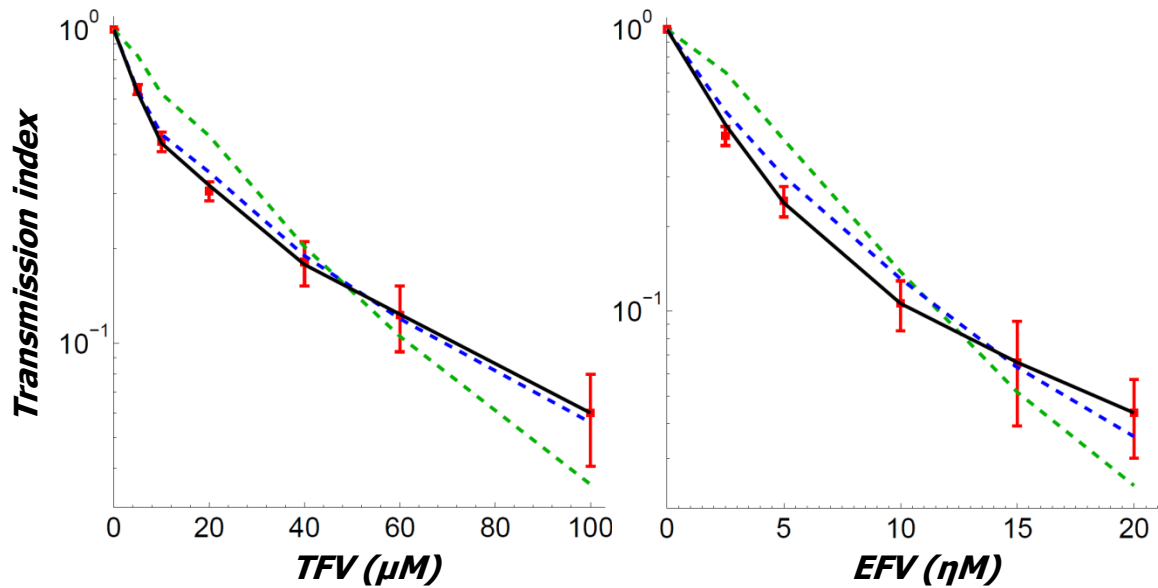


Figure S9: Decrease in drug sensitivity in coculture infection was not due to factors secreted by donor cells. To check whether infected cells in coculture might be secreting cytokines or other molecules that could modify the susceptibility of target cells to infection, we performed infections in transwell chambers, where infected MT-4mCherry donor cells were physically separated from the target cells, but molecule and virus exchange between compartments could occur. 5×10^5 Rev-CEM target cells were infected for 2 days by either coculture with 2×10^3 infected MT-4mCherry donor cells, or by cell-free virus generated by 2×10^5 MT-4mCherry donor cells across a membrane of a Corning HTS Transwell 24-well plate (polycarbonate, $0.4 \mu\text{m}$ pore size, cat# 3396). After 2 days of infection, 5×10^5 cells were analyzed for GFP expression by flow cytometry and fusions excluded. No mCherry positive cells or fusions were detected in infection across the transwell, indicating that infection occurred by diffusion of cell-free virus alone. Red squares: coculture. Blue Squares: infection across transwell barrier. Lines are guides for the eye. Means \pm s.d. of three consecutive independent inter-day experiments. Transwell infection maintained the higher sensitivity of cell-free infection to drug, indicating that the donor cells are not secreting factors that can decrease drug sensitivity.



Fits:	RMSE:		df:
	TFV	EFV	
— Two-peaked Poisson	0.02	0.01	3
⋯ Poisson	0.3	0.4	1
⋯ Log-normal	0.07	0.2	3

■ Experimental values from coculture

Figure S10: Two-peaked Poisson distribution results in closest fit for the number of infectious units transmitted in coculture. Fits of two-peaked Poisson (black line), single peaked Poisson (green line), and log-normal distributions (blue line) of m to the experimental data. Left panel shows fits for TFV, right panel shows fits for EFV. RMSE: Root mean squared error. df: Degrees of freedom in fit.

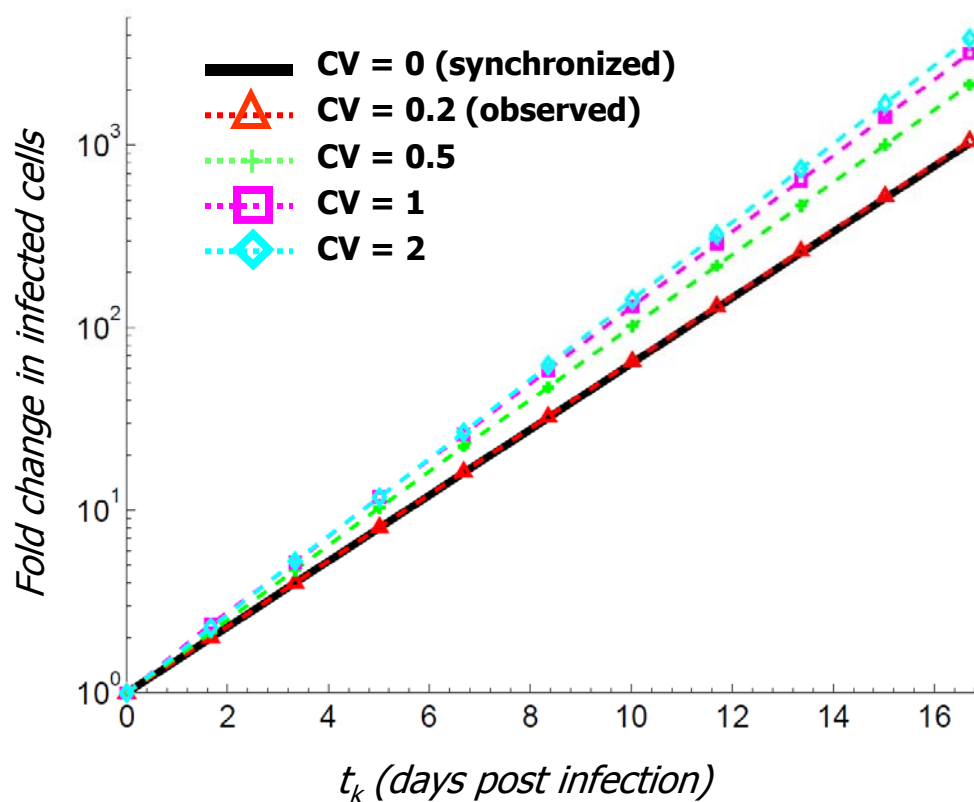


Figure S11: Simulated effect of desynchronization of viral reproductive cycles on infection growth rate. For each of 100 individual input donor cells at day 0, we calculated the number of total cells infected at each time point $t_n = n\tau$, where n is an integer and τ is the average virus cycle length, experimentally determined to be 1.7 days with a CV_τ (s.d./mean) of 0.2 (Fig. S2). Each infected cell at t_n generated R^k new infected cells at t_{n+1} , where R is the replication ratio and k is a random variable from a normal distribution with $\mu = 1$ and $\sigma = \mu CV_\tau$. Negative numbers of k , or k greater than the number of elapsed days (since virus cycles cannot be shorter than one day), were excluded. The sum of infected cells for each time point was divided by the number of input infected cells to obtain the fold change for that time point, and used as the number of donor cells for the next time point. Plot is for $R = 2$. Fold change in infected cells as a function of elapse time is shown for infection where simulated CV values were 0 (synchronized, black), 0.2 (experimentally observed, red), 0.5 (green), 1 (magenta), and 2 (cyan).

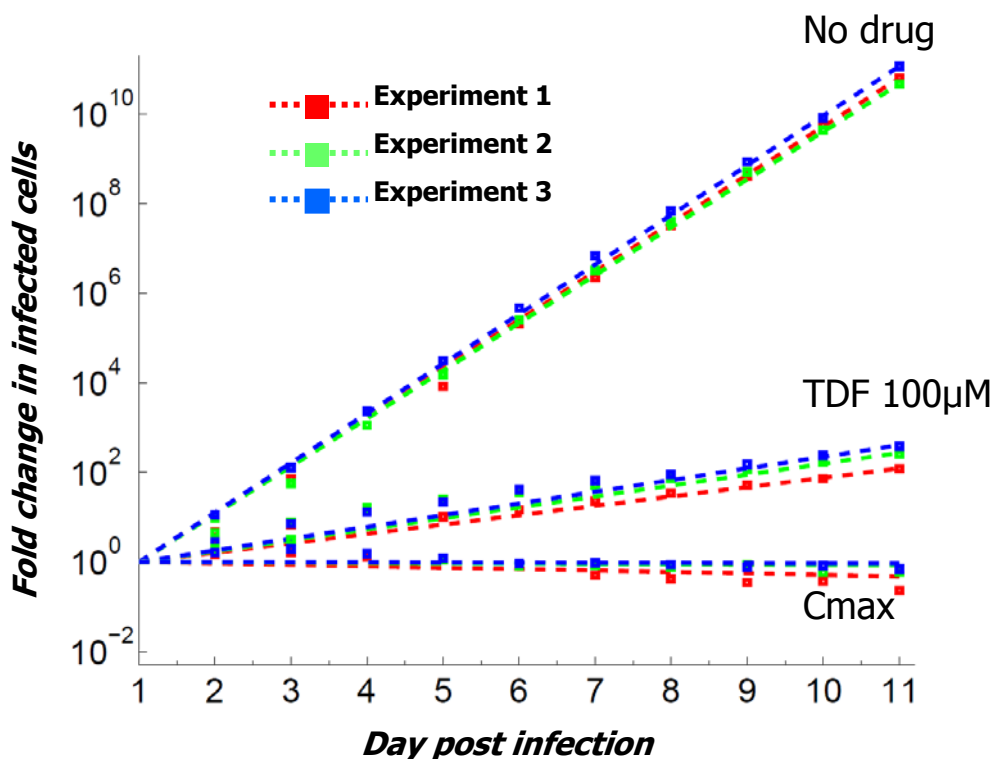


Figure S12: Fold change in the number of infected cells with time in individual independent inter-day experiments. Drug conditions were: no drug, 100 μM TFV, and Cmax (10 μM EFV, 2 μM TFV, and 10 μM FTC). Dashed lines represent fits of the equation $I_k = I_0 R^k$ for each drug condition. Replication ratios fit from the data were: Experiment 1: $R_{\text{no drug}} = 63$, $R_{\text{TFV}} = 2.2$, $R_{\text{Cmax}} = 0.89$. Experiment 2: $R_{\text{no drug}} = 60$, $R_{\text{TFV}} = 2.5$, $R_{\text{Cmax}} = 0.97$. Experiment 3: $R_{\text{no drug}} = 70$, $R_{\text{TFV}} = 2.7$, $R_{\text{Cmax}} = 0.99$. Mean R_{Cmax} was not significantly different from 1 ($p = 0.24$) but slightly lower than 1 in all experiments.

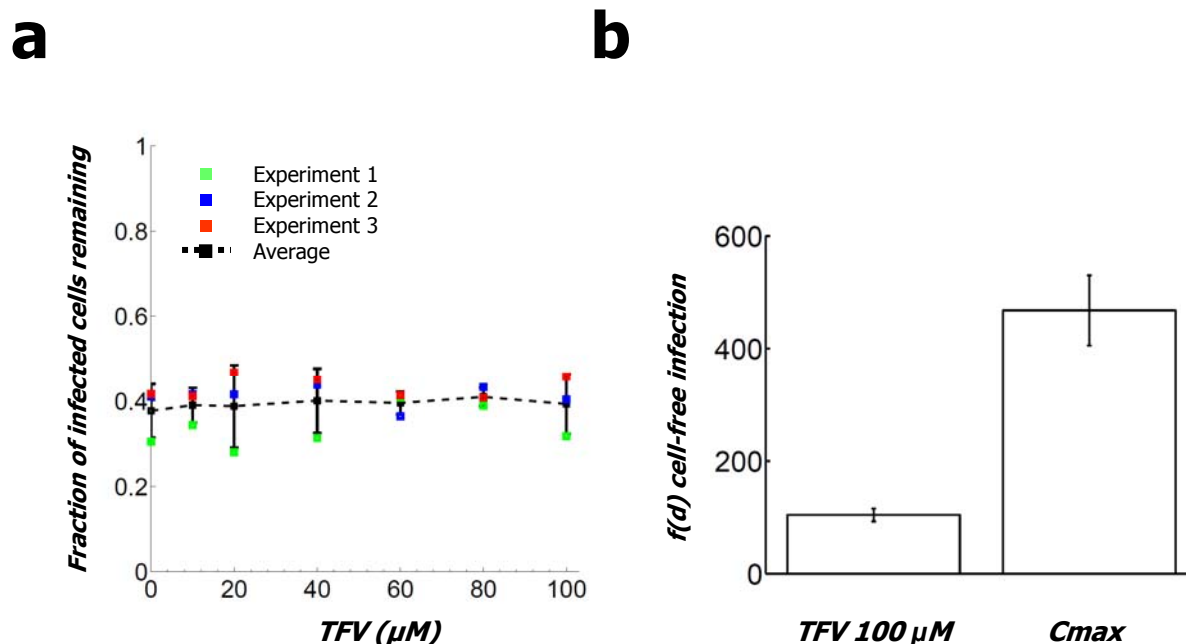


Figure S13: Data used to calculate $R_{TFVCellFree}$ and $R_{CmaxCellFree}$. Ratios were calculated using Eq. (3.7) (supplementary theory, Section 3). To find parameter values to calculate the theoretical cell-free infection ratios, we measured the half-life of virus producing cells (a), the drug effect on a single round of cell-free infection (b), the replication ratio without drug (Fig. 3a), and the virus replication cycle time (Fig. S2). a) Average infected Rev-CEM half-life. 1000 GFP positive Rev-CEM cells were mixed with 2×10^6 uninfected CEM-ss parental non-reporter cells and incubated for 2 days with varying concentrations of TFV. We assumed that under these conditions, few new Rev-CEM cells should be infected in the first infection cycle since any virus would be adsorbed by the large number of uninfected CEM-ss cells. This assumption is validated as increasing TFV concentrations did not change the number of GFP positive cells at day 2, indicating that negligible new infection of Rev-CEM targets occurred. Therefore, the difference between the number of GFP positive cells on day 0 versus day 2 post mixing is almost entirely because of HIV mediated cell death of infected cells during the incubation period after mixing. Graph shows the number of remaining GFP positive cells 2 days post mixing as a fraction of input, averaged over three inter-day experiments. The fraction of GFP positive cells averaged across drug concentrations was 0.4 ± 0.01 , which translates to an average half-life of 1.5 ± 0.04 days (average \pm s.d.). b) Effect of 100 μ M TFV and C_{max} on a single cycle of cell-free virus infection. Mean \pm s.d. ($n = 3$), with 10^6 cells collected per sample by FACS.

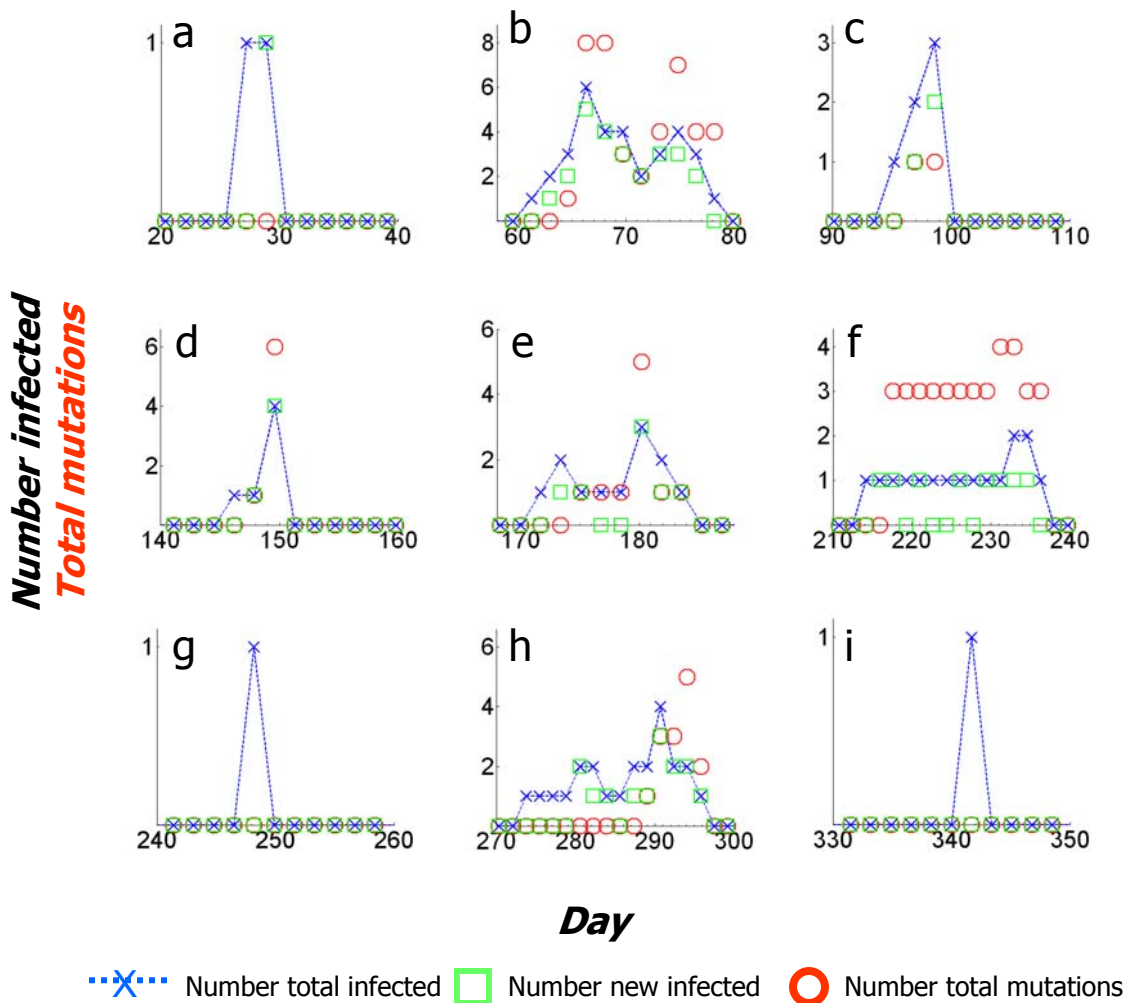


Figure S14: Representative individual infection chains. The number of newly infected cells was approximated as a random number from a Poisson distribution with a mean defined by the experimentally observed replication ratio for C_{max} . The probability of mutation if a new infection occurred was calculated as 0.29 (Methods). No fitness benefit or cost was assigned to individual mutations. Each infection chain arose with an input of one infected cell. In infection chains g and i, the input cell did not survive beyond the first infection cycle and caused no new infections. In infection chain a, the input cell infected one additional cell, but this infection did not lead to a mutation. The rest of the infection chains show more extensive infection but nevertheless terminate. Blue x's denote total infected cells, green squares denote the newly infected cells, and red circles denote the total number of mutations at each time point. The blue line connects the number of total infected cells and is a guide for the eye. Mutations could either be newly generated or carried over from the previous infection cycle if the mutated cell survived (Methods). Division at each time point of the sum of infected cells by the sum of mutations from all overlapping infection chains is presented as the bottom graph in Fig. 3b.

Sigal et al. supplementary theory

1 Relation of the number of transmitted viruses to drug sensitivity-deterministic case

1.1 Result

We define the transmission index (T_X) as the fraction of cells infected in the presence of drug divided by the fraction of cells infected in the absence of drug. Below we show that

$$T_X = \frac{I_d}{I} = \frac{1 - e^{-r\lambda/f(d)}}{1 - e^{-r\lambda}} = \frac{1 - e^{-m/f(d)}}{1 - e^{-m}}. \quad (1.1)$$

Variables and parameters:

- I = the fraction of infected target cells without drug.
- I_d = the fraction of infected cells in the presence of drug.
- r = the probability of a single virus infecting a cell.
- λ = the number of viruses entering one cell.
- m = the number of infectious units $r\lambda$.
- d = drug concentration.
- $f(d)$ = the fold reduction of r by drug concentration d .

1.2 Model of infection

When the fraction of infected target cells (I) is low relative to the total target cell population (T), I is a product of T and the probability that each target cell is infected:

$$I = T \cdot \text{Prob}(\text{infection per cell}). \quad (1.2)$$

The probability that no infection occurs per virus is $1 - r$. We assume that the infection probability per virus is independent of other virus infections. Hence given λ viruses contacting a single cell, the probability that none of the viruses infect is

$$\text{Prob}(\text{no infection by } \lambda \text{ viruses}) = (1 - r)^\lambda. \quad (1.3)$$

Therefore, the probability of successful infection with λ viruses per cell is $1 - (1 - r)^\lambda$ and the total number of infected cells is

$$I = T(1 - (1 - r)^\lambda). \quad (1.4)$$

1.3 Parameter values

Values for parameters above were measured in our experimental system for cell-free virus infection:

Table 1: Experimentally found quantities for cell-free virus infection

Quantity	Description	Found by	Value
V	number of input virus genomes	Abbott qPCR	10^{10}
I^1	number infected cells	flow cytometry	10^4
T^2	number target cells	flow cytometry	10^6
r^3	probability of infection	I/V	10^{-6}
λ^4	number viruses per cell	V/T	10^4

1.4 Model of infection with drug

Anti-HIV drug classes such as reverse transcriptase inhibitors, integrase inhibitors, and fusion inhibitors, interfere with the virus life cycle before successful infection. Therefore, they reduce infection frequency. These classes are considered here:

$$r \rightarrow \frac{r}{f(d)}. \quad (1.5)$$

The effect of infection inhibiting drugs on the number of infected cells is

$$I = T(1 - (1 - r/f(d))^\lambda). \quad (1.6)$$

The ratio of the number of infected cells with drug to the number of infected cells without drug is therefore

$$T_X = \frac{I_d}{I} = \frac{T(1 - (1 - r/f(d))^\lambda)}{T(1 - (1 - r)^\lambda)} = \frac{1 - (1 - r/f(d))^\lambda}{1 - (1 - r)^\lambda}. \quad (1.7)$$

Since it is known experimentally that $r \ll 1$, we can use the approximation $1 - x \approx e^{-x}$, $|x| \ll 1$, to rewrite Eq.(1.9) as

$$T_X \approx \frac{1 - e^{-(r/f(d))\lambda}}{1 - e^{-r\lambda}}. \quad (1.8)$$

¹Measured at the end of a 2 day experiment. Since the virus cycle time in our experimental system was on average 1.7 days, two days will capture the majority of infected cells without substantial infected cell death.

²Measured at the end of a 2 day experiment. This is the total number of infectable cells and includes infected cells, though latter is a negligible part of the total.

³Possible reasons that an input virus may not infect a cell and thus decrease r include virus degradation or loss of infectivity before reaching an infectable cell, the virus random walk never coming in contact with an infectable cell, more than one virus needed to infect a cell, and the virus failing to complete essential intracellular infection steps such as reverse transcription and integration.

⁴This is an upper estimate, the maximum number of viruses available per cell. The number of viruses actually entering each cell will be lower.

1.5 Limiting cases

For cell-free virus infection at the dilution shown in Table 1, $r\lambda \ll 1$. At this limit, we can use the approximation $e^x \approx 1 + x$ for $|x| \ll 1$ to arrive at

$$T_X \approx \frac{r\lambda/f(d)}{r\lambda} = 1/f(d). \quad (1.9)$$

Other limiting cases can be found by using the expansions $e^x \approx 1 + x$ for $|x| \ll 1$ and $e^{-x} \approx 0$ for $|x| \gg 1$, and the definition $r\lambda \equiv m$. These are listed below

- $m/f(d) \gg 1 \implies T_X \approx 1$.
- $m \gg 1 \implies T_X \approx 1 - e^{-m/f(d)}$.
- $m \gg 1, m/f(d) \ll 1 \implies T_X \approx m/f(d)$.

2 Relation of the number of transmitted viruses to drug sensitivity-stochastic case

The number of viruses, λ , is more realistically treated as a random variable sampled from a distribution. Let $p(\lambda)$ be that distribution. Then the observed T_X is the ratio of the averages

$$\bar{T}_X(f(d)) = \frac{\int (1 - (1 - r/f(d))^\lambda) p(\lambda) d\lambda}{\int (1 - (1 - r)^\lambda) p(\lambda) d\lambda}. \quad (2.1)$$

Here we assumed that the drug does not affect the distribution and that λ varies continuously (in the discrete case the integral is replaced by a sum). Using the normalization condition for the probability distribution function $\int p(\lambda) d\lambda = 1$ we can be further simplify the expression for $\bar{T}_X(f(d))$ as follows:

$$\bar{T}_X(f(d)) = \frac{1 - \int (1 - r/f(d))^\lambda p(\lambda) d\lambda}{1 - \int (1 - r)^\lambda p(\lambda) d\lambda}. \quad (2.2)$$

An approximate value can be found in the limit $r\lambda \ll 1$. Expanding $(1 - r)^\lambda$ in r around 0 up to first order,

$$(1 - r)^\lambda = 1 - r\lambda + O(r^2). \quad (2.3)$$

and substituting back into $\bar{T}_X(f(d))$ we get

$$\bar{T}_X(f(d)) = \frac{1 - \int (1 - r\lambda/f(d)) p(\lambda) d\lambda}{1 - \int (1 - r\lambda) p(\lambda) d\lambda} = \frac{\int (r\lambda/f(d)) p(\lambda) d\lambda}{\int r\lambda p(\lambda) d\lambda} = \frac{1}{f(d)}. \quad (2.4)$$

which reproduces our result in equation 1.10 above. In the general case $\bar{T}_X(f(d))$ can be compared numerically with the experimentally found dependence. However, in some special cases an exact analytical expression for \bar{T}_X can be found. One of these is if λ is sampled from a Poisson distribution with mean μ , that is

$$p_\mu(\lambda) = \frac{\mu^\lambda e^{-\mu}}{\lambda!}. \quad (2.5)$$

Accordingly the probability for infection with λ viruses is

$$I(\lambda; \mu, r) = T(1 - (1 - r)^\lambda) \frac{\mu^\lambda e^{-\mu}}{\lambda!}. \quad (2.6)$$

Summing over λ we get

$$I(\mu, r) = T \sum_{\lambda=0}^{\infty} I(\lambda; \mu, r) = T \sum_{\lambda=0}^{\infty} (1 - (1 - r)^\lambda) \frac{\mu^\lambda e^{-\mu}}{\lambda!}. \quad (2.7)$$

Expanding the parenthesis and noting that $\sum_{\lambda=0}^{\infty} \mu^\lambda e^{-\mu} / \lambda! = 1$ we arrive at

$$I(\mu, r) = (1 - e^{-\mu} \sum_{\lambda=0}^{\infty} \frac{((1 - r)\mu)^\lambda}{\lambda!}) T. \quad (2.8)$$

Finally, recognizing that $\sum_{n=0}^{\infty} z^n / n! = e^z$ we arrive at our key result:

$$I(\mu, r) = (1 - e^{-\mu} e^{(1-r)\mu}) T = (1 - e^{-r\mu}) T. \quad (2.9)$$

Accordingly T_X takes the same form as the deterministic solution

$$T_{X\mu}(f(d)) = \frac{I_d}{I} = \frac{1 - e^{-(r/f(d))\mu}}{1 - e^{-r\mu}}. \quad (2.10)$$

Note that this result is valid for both the drug classes that reduce infection frequency and burst size since in both cases the drug effect reduces the mean of the distribution, $\mu \rightarrow \mu/f(d)$.

3 Calculating predicted infection behavior of cell-free virus in the presence of drugs

Whether infection expands or terminates depends on the replication ratio R [1,2] which we define as

$$R = \sqrt[k]{\frac{I_k}{I_0}}, \quad (3.1)$$

where I_k is the number of infected cells at infection cycle k , and I_0 is the number of infected cells at the start of the experiment. If $R > 1$, the infection expands. If $R < 1$, the infection eventually terminates. We wish to obtain R_{free}^d , the replication ratio for cell-free virus in the presence of drug. However, infection for multiple infection cycles is a combination of cell-free and cell-to-cell transmission so that R_{free}^d cannot be measured. R_{free}^d can still be predicted if its relationship to R , the measurable replication ratio without drug, and $f_{free}(d)$, the drug effect per cell-free virus infection cycle, can be established. We derive that relationship below.

In the case where the number of uninfected cells is non-limiting (approximated in our experiments by keeping the fraction of infected cells low), the number of infected cells in the $(k+1)$ -th cycle of infection depends both on the number of newly infected cells, infected by cells from the k -th cycle, and the number of infected cells remaining from the k -th cycle.

$$I_{k+1} = I_{k+1}^{new} + I_{k+1}^{leftover}. \quad (3.2)$$

The number of newly infected cells is determined by ρ , where $\rho \propto r\lambda$ [1]:

$$I_{k+1}^{new} = \rho I_k. \quad (3.3)$$

For simplicity, we assume that ρ is identical for any two consecutive cycles. The number of infected cells left over from the k -th cycle is:

$$I_{k+1}^{leftover} = 2^{-\frac{\tau}{t_{1/2}}} I_k. \quad (3.4)$$

Where τ is the virus cycle length, and $t_{1/2}$ is the infected cell half-life after it starts producing virus. Therefore, the equation for the number of infected cells in the $(k+1)$ -th cycle as a function of the number of infected cells in the k -th cycle is

$$I_{k+1} = \rho I_k + 2^{-\frac{\tau}{t_{1/2}}} I_k. \quad (3.5)$$

The first term takes into account the rate of addition of newly infected cells and the second term takes into account the number of cells left over from the previous virus infection cycle. Eq.(3.5) can be easily solved for I_k as a function of the initial infected cells at start I_0 . If $q = \rho + 2^{-\frac{\tau}{t_{1/2}}}$, it can be seen that $I_1 = I_0 q$, $I_2 = I_1 q = I_0 q^2$, $I_k = I_0 q^k$. We therefore obtain

$$I_k = I_0 \left(\rho + 2^{-\frac{\tau}{t_{1/2}}} \right)^k. \quad (3.6)$$

Eq (3.6) can be used to fit infection dynamics with no drug to obtain ρ . To find the predicted infection replication rate for cell-free virus with drug, we use Eq (1.5) or Eq (1.6) and the relation $\rho \propto r\lambda$ [1,2] to obtain $\rho_d = \frac{\rho}{f(d)}$, where ρ_d is ρ in the presence of drug. Substituting into Eq (3.6) gives the replication rate as a function of I_k^d , the number of infected cells with drug at infection cycle k , ρ , and the drug effect $f_{free}(d)$:

$$R_{free}^d = \sqrt[k]{\frac{I_k^d}{I_0}} = \frac{\rho}{f_{free}(d)} + 2^{-\frac{\tau}{t_{1/2}}}. \quad (3.7)$$

Table 2 lists numerical values for the parameters appearing in Eq (3.7) and their sources.

Table 2: Values of components for Eq (3.7)

Quantity	Value	Found by
ρ	64	Fit of infection without drug to Eq (3.6)
$f_{free}(TFV)$	1×10^2	$1/T_X$ for $100 \mu M$ TFV for drug stock used in experiment
$f_{free}(Cmax)$	5×10^2	$1/T_X$ for $10 \mu M$ EFV + $2 \mu M$ TFV + $10 \mu M$ FTC for drug stocks used in experiment
τ	1.7	Measured, Fig. S4
$t_{1/2}$	1.5	Measured, Fig. S13

References

- [1] Ribeiro, R. M., Qin, L., Chavez, L. L., Li, D., Self, S. G., and Perelson, A. S. Estimation of the initial viral growth rate and basic reproductive number during acute HIV-1 infection. *J Virol.* 2010 Jun;84(12):6096-102.
- [2] Nowak, M.A., and May, R.M. *Virus dynamics : mathematical principles of immunology and virology.* Oxford University Press, 2000.